

PAPER • OPEN ACCESS

A Comparison of the Characteristics of Extreme Drought During the Late 20th and Early 21st Centuries Over Eurasia and North America

To cite this article: A R Lupo *et al* 2022 *IOP Conf. Ser.: Earth Environ. Sci.* **949** 012122

View the [article online](#) for updates and enhancements.

You may also like

- [Divergent responses of ecosystem water use efficiency to drought timing over Northern Eurasia](#)
Mengtian Huang, Panmao Zhai and Shilong Piao
- [An emerging impact of Eurasian spring snow cover on summer rainfall in Eastern China](#)
Taotao Zhang, Tao Wang, Yingying Feng et al.
- [Possible contribution of heavy pollution to the decadal change of rainfall over eastern China during the summer monsoon season](#)
Yang Zhou, Jing Jiang, Anning Huang et al.



ECS The Electrochemical Society
Advancing solid state & electrochemical science & technology

241st ECS Meeting

Vancouver, BC, Canada. May 29 – June 2, 2022

ECS Plenary Lecture featuring
Prof. Jeff Dahn,
Dalhousie University

Register now!

A Comparison of the Characteristics of Extreme Drought During the Late 20th and Early 21st Centuries Over Eurasia and North America

A R Lupo^{1,*}, N K Kononova², I G Semenova³ and M G Lebedeva⁴

¹ Atmospheric Science Program and Missouri Climate Center, School of Natural Resources, University of Missouri, Columbia, MO 65211, USA

² Institute of Geography, Russian Academy of Sciences, Moscow 119017, Russian Federation.

³ Department of Military Training, Odessa State Environmental University, Odessa, Ukraine.

⁴ Department of Geography and Geoecology, Belgorod State University, Belgorod 308015, Russia

* E-mail: lupa@missouri.edu

Abstract: The atmospheric general circulation character during summer droughts over Eastern Europe / Western Russia and North America from 1970 – 2020 is examined here. A criterion to examine atmospheric drought events encompassed the summer season was used to determine which years were driest using precipitation, evaporation, and areal coverage. The relationship between drought and atmospheric character using the Dzerzevsky climatic classification scheme, atmospheric blocking, teleconnections, and information entropy are used to study the atmospheric dynamics. The National Centers for Environmental Prediction (NCEP) re-analyses data set archived at the National Center for Atmospheric Research (NCAR) in Boulder, CO, USA is used to examine the synoptic character and calculate the dynamic quantities for these dry events. The results demonstrate that extreme droughts over North America are associated with a long warm and dry period of weather and the development of a moderate ridge over the central USA driven by surface processes. Extreme droughts over Eastern Europe and Western Russia are driven by the occurrence of prolonged blocking episodes as well as surface processes.

1. Introduction

Drought is a complicated, interdisciplinary problem studied extensively in recent years, especially in connection with climate change (e.g., [1]), and impacts more people than any other natural hazard [1]. Drought can be classified as agricultural, hydrological, and meteorological and these definitions are found in meteorological textbooks (e.g., [2]). Drought can impact on important phenological times in agriculture [3], [4]. For example [3], demonstrated the reproductive stage of the growing season for corn and soybean in the central United States (USA) is July and August. Then [4] shows the impact of dry periods on winter and spring wheat in the Missouri River Basin.

Over North America (NA) for example, [5] attributed the drought of 1980 to an accentuated and persistent upper air (500 hPa) ridge, and troughs off the Pacific and Atlantic coasts. This drought was preceded by cooler sea surface temperature (SSTs) anomalies over the central tropical Pacific for two



seasons previous to the drought, and the 500 hPa flow pattern was established by spring. This drought is memorable for the impact on agriculture and the economy of the USA (e.g. [5]). Later, [6] supported [5] regarding the precursor 500 hPa pattern and identified an unusual Pacific North American (PNA) teleconnection associated with a shorter wavelength. The work of [7 -9] found prominent SST patterns varied in association with interannual (e.g., El Niño and Southern Oscillation – ENSO) and interdecadal variability (e.g., Pacific Decadal Oscillation - PDO) impacting the weather and climate of the central USA. Henson et al. [10] studied the relationship between interannual and interdecadal variability of Pacific Region SSTs, growing season conditions, and corn and soybean yields in the Missouri. They found yields were generally less during the transition toward La Niña years as these were associated with warmer and drier summers.

A series of dry years has been observed within Eastern Europe and Western Russia (EE/WR) over the last 15 years (e.g., [11]). Ionita et al [11] demonstrated past ‘megadrought epochs’ over central Europe were decadal. However, [12] found the trend in drought over central and eastern Europe has been steady since the mid-20th century. In the southern East European plain, Cherenkova et al. [13] demonstrated the average yield for winter wheat, spring wheat and spring barley in the westerly Quasi-biennial Oscillation (QBO) phase exceeded the same yield for the eastward QBO. The 2010 drought in eastern Europe and Russia has been attributed to summer blocking episodes (e.g., [14]) This work [14] associated five well-known dry and wet years with ENSO variability across the region. They linked the transition of ENSO with dry summers. Then [15] linked the warmer drier climate of southwestern Russia with the increase in certain weather types including blocking.

The association of Northern Hemisphere (NH) weather types with dry and wet periods was championed by N.K. Kononova (e.g., [16, 17]). These NH weather types, termed elemental circulation mechanisms (ECMs), was first proposed by [18]. This work [18] proposed 13 different NH flow types and 41 sub-types based on the amplitude, location, and number of waves on the polar front jet stream [19], which could be grouped into four general NH flow types, two zonal and two meridional types. Further, [16, 17] would associate an epoch of zonal flow during the early to mid-20th century with the dry years over NA and parts of Russia during the 1930s. The relationship between these ECM and NH teleconnection activity as well as the theoretical work of Lorenz and others was discussed in [20]. Also, [19] demonstrated the concept of Information Entropy could be applied to the occurrence of zonal versus meridional NH flow types. This ECM classification is convenient for the definition of synoptic processes influencing the occurrence of regional weather hazards often related to drought, such as a dry hot wind, which is called “*Sukhovey*” in Ukraine and Russia [21]. They may accompany droughts, but they are also associated with the periphery of anticyclones. Droughts in this region usually occur within the central part of a large-scale anticyclones [22].

The goal here is to examine the occurrence of summer drought from 1970 – 2020 over agriculturally sensitive regions of NA and EE/WR. This study uses an objective criterion for summer drought based on precipitation and potential evaporation anomalies as well as the amount of area impacted. The occurrence of summer drought will be related to long term atmospheric variability, the occurrence of atmospheric blocking, and the occurrence of ECMs. This work also examines whether drought in each region is associated with precursors and differentiate between the atmospheric character of extreme drought summers versus moderate drought summers.

2. Data and Methods

The NH 500 hPa height, precipitation rate (mm day^{-1}) (P), and potential evaporation (W m^{-2}) (E) data were retrieved from the National Centers for Environmental Prediction (NCEP)/National Center for Atmospheric Research (NCAR) reanalyses [23] available through the NOAA Earth System Research Laboratory (ESRL) at 6 h time intervals on a 2.5° latitude by longitude grid from 1948–2020. The potential evaporation data were converted to mm day^{-1} by dividing E by the latent heat of vaporization ($L = 2.5 \times 10^6 \text{ J kg}^{-1}$) and the density of water (1000 kg m^{-3}). The study period was 1970 – 2020.

The atmospheric blocking information was obtained from the blocking archive housed in the University of Missouri Weather Analysis and Visualization (WAV) laboratory [24]. The blocking

information used was duration (days) and intensity (BI) and is available from 1968 to 2021. Blocking events in the EE/WR were examined consistent with [14] and [25] (20° – 60° E). Blocking is rare over NA [6], [26]). Extreme weather over NA, especially the central region, has been associated with blocking over the eastern North Pacific (e.g., [27]), defined as 180° – 100° W [26, 27]. The teleconnection indexes, such as the Arctic Oscillation, the North Atlantic Oscillation (NAO), and PNA were downloaded from the Climate Prediction Center website [28] and were chosen since they are commonly associated with weather and climate in the study regions. Also, the AO shows correspondence with zonal versus meridional ECM groups (e.g., [20]).

The daily classifications of the ECM and their monthly and annual statistics since 1899 are available via the Russian Academy of Sciences, Institute of Geography website [29]. A description and the history of ECM are found in [16-20], and included four circulation groups displayed in Table 1 of [19]. Then [32] used 500 hPa maps when these became routinely available in the late 1940s, and [19], [20] show maps of the NH ECM groups.

The Japanese Meteorological Agency (JMA) definition for ENSO is described in [30] and the years are given in Table 1. The JMA index is available via the Center for Ocean and Atmospheric Prediction Studies (COAPS) from 1868 to present [30]. The JMA classifies ENSO phases using SST within the Niño 3.4 region, and defines an ENSO year as 1 October to 30 September.

Table 1. List of ENSO years used here. The years below are taken from [26] and [30].

El Niño (EN)	Neutral (NEU)	La Niña (LN)
1969	1968	1967
1972	1977-1981	1970-1971
1976	1983-1985	1973-1975
1982	1989-1990	1988
1986-1987	1992-1996	1998-1999
1991	2000-2001	2007
1997	2003-2005	2010
2002	2008	2017
2006	2011-2013	2020
2009	2016	
2014-2015	2019	
2018		

Over NA, the study box is bounded by 30° N and 50° N, and 100° W and 80° W. This includes much of the corn, wheat, soybean belts in NA (e.g., [4], [10]). Over EE/WR, this box is bounded by 40° N and 60° N, and 20° E and 50° E, which includes the major wheat growing regions of EE, Ukraine, and WR. Soybeans, corn, sugar beet, and sunflower are primary crops of southwestern Russia. In Ukraine, winter wheat, spring barley, (these are 90-95% of the crop area) and corn are the main grain crops. Sunflowers and sugar beets are also major crops. Corn is the third most important feed grain, planted in eastern and southern Ukraine [31].

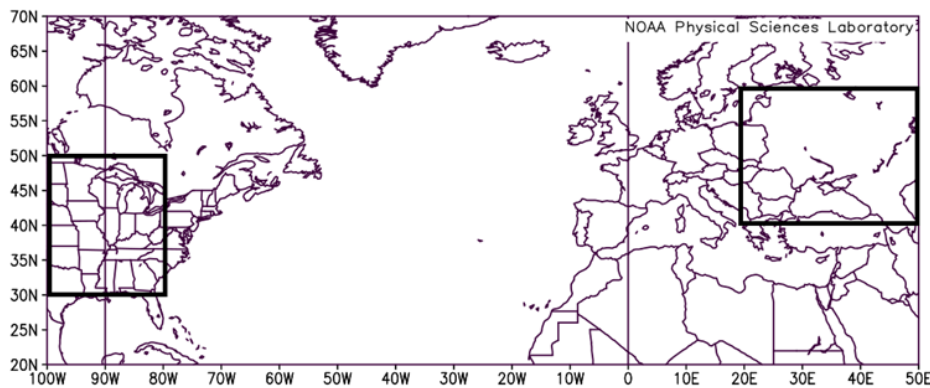


Figure 1. The study regions used here.

This drought definition [25] is used and the criterion are; 1) the largest difference between a maximum P anomaly (mm day^{-1}) and a E anomaly (mm day^{-1} - near the former), and 2) the areal coverage of the negative P anomaly. If criterion one was greater than -9 mm day^{-1} , the year was an extreme drought. If criterion one was less than -9 mm day^{-1} and the areal extent was larger than $1.893 \times 10^6 \text{ km}^2$ (50% of the NA region / 40% of the EE/WR), year was considered a moderate drought year. The extreme (moderate) drought sample size was ten and eight (12 and eight) years for the NA and EE/WR study regions. The total area of the NA region is $3.786 \times 10^6 \text{ km}^2$ and the EE/WR region is $4.765 \times 10^6 \text{ km}^2$, thus the latter region is approximately 25% larger.

Then [19] used Shannon or Information Entropy (IE) to discuss the occurrence of zonal versus meridional flows. Type 1 and Type 2 (Type 3 and Type 4) flows were considered zonal (meridional) NH flow regimes. The formula used for IE was:

$$H(x) = -\sum_{i=1}^n p(x_i) \log_b p(x_i) \quad (1)$$

where b is the base logarithm and $p(x)$ is the probability of a certain outcome. Entropy is described as a measure of predictability, structure, or organization within a system [19]. As described in [19], the IE for the NH observed flow would be 0.99 if all 41 of the NH flow ECM types of [18] were equally likely. The observed IE based on all years from [19] was 0.90, and the years since the late 20th century and early 21st century were 0.76 and 0.57, respectively. Here we examine spring and summer values of IE, which was not done in [19].

3. Results

An examination of NA summer drought showed 13 of the 22 years occurred during the decade of the 1970s and 2010s (Table 2). In the EE/WR, 8 of 16 summer droughts occurred during these decades. The extreme summer droughts occurred most often during the 1970s for NA and the 2010s for EE/WR. In the latter, drought was related teleconnections such as the AMO (e.g., [11]), PDO (e.g., [15]), or interdecadal variability of blocking [26]. In the NA, the earlier decade overlaps with the PDO changeover from negative (1949 – 1976) to positive (1977 – 1998). For the later decade it is not clear the PDO has changed from the current negative phase, and [1] and [10] found the negative PDO years in the NA were drier.

Table 2. The occurrence of extreme and moderate NA drought. Columns 1,2, and 3 show the maximum P minus E (mm day^{-1}), the percent of the region covered by -1 mm day^{-1} or greater P-E, and the product of the column 2, 3 / rank, respectively. Columns 4 and 5 show the ENSO phase and whether the preceding spring showed drought conditions, respectively.

Year	P-E Anomaly	% area covered	Column 2 x 3 / Rank	ENSO Phase	Precursor
Extreme					
1972	-14.5	60	-8.7 / 2	LN	Yes
1976	-9.0	90	-8.1 / 3	LN	Yes
1978	-9.0	70	-6.3 / 6	NEU	Yes
1980	-14.0	75	-10.5 / 1	NEU	Yes
1982	-10.0	25	-2.5 / 21	NEU	No
1990	-11.0	40	-4.4 / 9	NEU	Yes
1998	-9.0	40	-3.6 / 14	EN	Yes
2000	-10.0	75	-7.5 / 4	LN	Yes
2011	-13.5	30	-4.1 / 12	LN	Yes
2012	-9.0	30	-2.7 / 20	NEU	Yes
Moderate					
1970	-7.0	75	-5.3 / 7	EN	Yes
1973	-7.0	60	-4.2 / 10	EN	No
1974	-8.0	85	-6.8 / 5	LN	Yes
1975	-5.0	50	-2.5 / 22	LN	No
1977	-7.0	55	-3.9 / 13	EN	Yes
1985	-5.0	60	-3.0 / 18	NEU	Yes
1988	-7.0	50	-3.5 / 15	EN	Yes
1999	-6.0	70	-4.2 / 11	LN	Yes
2006	-5.0	60	-3.0 / 19	NEU	Yes
2015	-7.0	50	-3.5 / 16	EN	No
2017	-5.5	60	-3.3 / 17	NEU	No
2020	-8.0	60	-4.8 / 8	NEU	No

When examining ENSO variability over NA (Table 2), four of 10 extreme summer droughts were associated with LN years. If moderate drought years are included, seven of 11 LN (22% of all years) were drought years. On the other hand, five moderate summer drought years were EN years (14 total years - 27%). However, when testing these distributions using Chi-square goodness of fit test [33] only the extreme summer drought distribution is different from the total sample (not at standard levels of significance). In the NA, [8] shows EN years and LN years during the negative PDO are dry. These results are consistent with extreme drought summers occurring during LN and NEU years, and moderate dry summers occurring over more than 50% of the NA [8].

Table 3. As in Table 2, except for EE/WR. Column 4 was multiplied by 0.8 to normalize this area to the area from Table 2.

Year	P-E Anomaly	%area covered	col 2 x 3 / rank	ENSO Phase	Precursor
Extreme					
1972	-9.0	30	-2.2 / 12	LN	No
1992	-10.0	70	-5.6 / 4	EN	Yes
1994	-10.0	80	-6.4 / 3	NEU	Yes
2002	-10.0	70	-5.6 / 5	NEU	Yes
2008	-9.0	35	-2.0 / 14	LN	No

2010	-11.5	50	-4.6 / 6	EN	No
2015	-10.5	80	-6.7 / 1	EN	No
2017	-10.0	80	-6.4 / 2	NEU	Yes
Moderate					
1971	-5.5	40	-1.8 / 16	LN	Yes
1975	-5.5	40	-1.8 / 15	LN	Yes
1979	-5.0	50	-2.2 / 13	NEU	Yes
1993	-7.0	40	-2.2 / 11	NEU	Yes
1996	-5.0	75	-3.0 / 8	NEU	Yes
2000	-8.0	40	-2.6 / 9	LN	No
2009	-7.0	40	-2.2 / 14	NEU	Yes
2020	-8.0	65	-4.2 / 7	NEU	Yes

Within the EE/WR (Table 3), there is a toward EN years for extreme summer drought, while the opposite was true for moderate summer drought. Spatially, for the extreme summer droughts, the precipitation deficit was larger in the northern EE/WR, while the opposite was generally true for moderate summer droughts (not shown, also [14]). The statistical test was applied for EE/WR and the moderate drought summer distribution was not the same as the total but not at standard levels of significance. In Tables 2 and 3, a majority of the summer drought years in both regions were preceded by a dry spring, but only half of these for extreme drought in the EE/WR. The results of [14] concluded summer droughts were not necessarily preceded by a dry spring in the EE/WR, but was biased by their small sample size.

Table 4. Spring sample groups from Tables 2 and 3 are in column one, the mean number of blocking events (occurrences / days / BI) in column two, the major NH teleconnections (AO / NAO / PNA) in column three, and the mean occurrences of ECM and IE (% zonal / % meridional / entropy). Bold (*, **) values represent statistical significance at $p = 0.1$ ($p = 0.05$, $p = 0.01$), respectively.

Sample	Blocking	Teleconnections	ECM / Entropy
NA extreme dry	1.9 / 17.1 / 3.81	0.40 / 0.37 / -0.16	19.8 / 80.2 / 0.72
NA moderate dry	2.2 / 17.6 / 3.65	0.11 / -0.13 / -0.15	20.0 / 80.0 / 0.72
NA wet	4.1* / 35.0 / 3.23	-0.18 / -0.04 / 0.17	18.6 / 81.4 / 0.69
EE/WR extreme dry	2.5 / 24.4 / 3.09	0.35 / 0.32 / -0.01	13.7 / 86.3 / 0.58*
EE/WR moderate dry	2.6 / 23.0 / 2.78*	0.02 / -0.08 / 0.22	20.7 / 79.3 / 0.74
EE/WR wet	2.5 / 20.2 / 3.18	-0.01 / 0.04 / -0.13	21.1 / 78.9 / 0.74

Neither [17] or [19] examined the seasonal frequency of zonal and meridional NH flow epochs during spring and summer. If each of the ECM [18] were equally likely, then the frequency for zonal to meridional ECM would be 0.46 to 0.54, but [19] observed this to be 0.31 to 0.69 from 1899-2019, yielding a value of 0.90 for the IE. From 1970 – 2020, the frequency of occurrence for zonal to meridional flows was 0.20 to 0.80 and the IE was 0.73 which is similar to the 1899-2019 distribution [24] at $p = 0.1$ using the Kolmogorov-Smirnov or Chi-Square goodness of fit test [25]. The occurrence for zonal to meridional flows during spring and summer were 0.18 to 0.82 and 0.25 to 0.75, respectively. The IE was 0.68 and 0.82, respectively, but the difference is not statistically significant.

During the NA springs (Table 4), the occurrence of zonal versus meridional NH flows or ECM for extreme and moderate drought years as well as wet years was similar to those of spring overall from 1970 – 2020. There were fewer Pacific Blocking events (Table 4) and a negative PNA Index in NA for drought springs. But for the springs preceding wet summers, the PNA Index is positive and there was significantly more blocking.

During the spring preceding the extreme summer drought for the EE/WR study region was the NH flow more meridional relative to other springs at a statistically significant level ($p=0.05$) (Table 4). This is reflected in a strongly positive NAO and AO, and [20] demonstrated correspondence between these indexes. The correlations between the AO and NAO are high here for spring and summer subsample in Table 4 ($p=0.01$). There is also a negative correlation between the AO and PNA at $p = 0.05$, but only for extreme and moderate dry springs and summers. In the EE/WR, the NAO is weakly negative for springs preceding moderate drought summers Table 4.

Table 5. As in Table 4, except for the summer sample groups from Table 2 and 3, and the maximum P (mm day⁻¹) and absolute values 500 hPa (m) anomalies in column five.

Sample	Blocking	Teleconnections	ECM / Entropy	anomalies
NA extreme dry	0.4*/2.9*/ 1.91**	-0.15 / -0.32 / -0.23	31.7 / 68.3 / 0.90**	-3.9 / 18.2
NA moderate dry	1.1 / 8.9 / 2.52	-0.03 / -0.10 / 0.35	30.4 / 69.6 / 0.89**	-2.8 / 22.5
NA wet	1.1 / 12.1 / 2.53	-0.04 / 0.00 / 0.12	23.8 / 76.2 / 0.79	
EE/WR extreme dry	2.6 / 28.4 / 2.43	0.11 / -0.08 / 0.21	21.9 / 78.1 / 0.76	-3.1 / 53.3
EE/WR moderate dry	1.5 / 12.9 / 2.05	-0.15 / -0.15 / -0.12	27.4 / 72.6 / 0.85**	-2.4 / 26.0
EE/WR wet	2.1 / 18.0 / 2.14	-0.00 / 0.03 / 0.06	35.9 / 64.1 / 0.94**	

During the summer (Table 5), the occurrence of zonal NH flow regimes during extreme and moderate NA drought and wet seasons was consistent with summers overall. For all NA drought summers, the flow was more zonal and this result was significant at $p = 0.01$. The extreme drought summers were accompanied by larger maximum precipitation anomalies than moderate drought summers, but the absolute value of the maximum 500 hPa height anomalies were of similar strength. The extreme dry years (Fig. 2a) featured a positive 500 hPa height anomaly within the study region continuing the negative PNA values from Table 4. This is accompanied by significantly fewer ($p = 0.05$) and weaker ($p = 0.01$) blocking events in association with a strong Aleutian Low (Fig. 2a). Note the troughs off each coast of NA supporting [6]. For moderate droughts (Fig. 2c), the pattern changes to a positive PNA pattern. The positive 500 hPa height anomaly is now over the western NA which strengthens the climatological ridge located there (not shown). This places the study region in the convergent region between a 500 hPa trough and ridge with high pressure at the surface. In both cases (Fig. 2a,c), the PNA pattern has a shorter wavelength for dry summers [6]. Last, there is a strong trough over the eastern 2/3 of USA for wet summers (Fig. 2e), supporting the results of [8].

In the EE/WR (Table 5) the extreme dry summers were meridional over the entire NH, but more zonal during moderate drought and wet years ($p=0.01$). Like the NA, the maximum precipitation anomalies are larger during the extreme drought summers than for moderate drought summers. However, the maximum 500 hPa height anomalies for both drought groups were larger overall than over NA. Several studies (e.g., [15], [17], [20], [22]) showed the EE/WR has been associated with an increase in the occurrence of meridional NH ECM flow regimes, especially during summer (Table 5). The EE/WR has also been associated with an increase in atmospheric blocking [14], [15], [17], [20-22] and drought studies associated with the extreme summer drought of 2010 with atmospheric blocking.

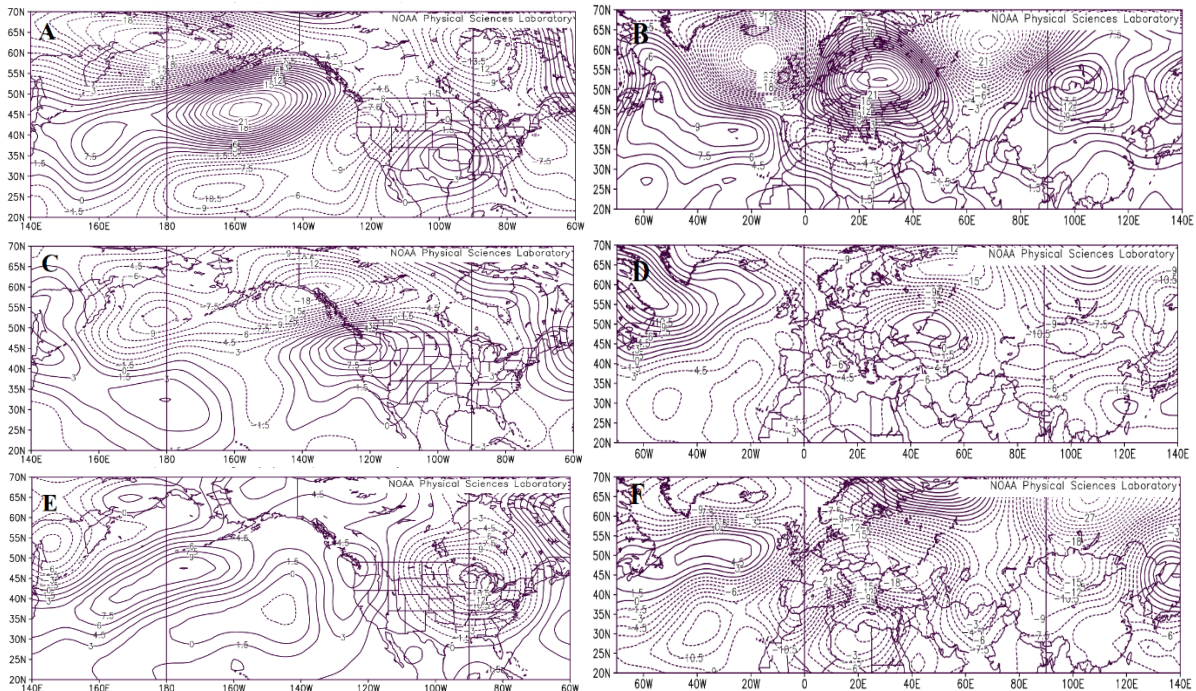


Figure 2. The 500 hPa height anomalies (m) in the a), c), e) NA and b), d), f) EE/WR during the summer (June – August – Table 2) a), b) extreme drought, c), d) moderate drought, and e), f) wet summers. The solid (dashed) lines are positive (negative) height anomalies. The contour interval is 1.5 m.

During the summer (Table 5), extreme droughts were associated with more blocking events and days significant at $p = 0.10$, while moderate droughts were associated with fewer blocking events, blocking days, and weaker events, significant at $p = 0.10$. These results are consistent with the interannual variability of blocking versus ENSO in the Atlantic [26]. Also, during EE/WR extreme drought summers, a strong negative Eurasian (EU) pattern (Fig. 2b) [34] was present continuing from spring, with the strongest positive anomaly over EE / WR. A negative EU is characterized by a positive 500 hPa height anomaly near 20° E and 145° E and a trough near 75° E. The negative EU during extreme dry summers are reminiscent of the quasistationary subseasonal and seasonal Rossby Wave trains accompany teleconnections in other parts of the globe (e.g., [34], [35]). During wet summers (Fig. 2f), the EU pattern is positive. Moderate drought years are associated with a negative NAO similar to the spring, but the EU pattern becomes less organized (Fig. 2d). The reversal of NAO in spring may indicate an extreme dry summer versus a moderately dry summer with a weakly negative EU.

The discussion above implies atmospheric dynamics are the primary drivers of summer drought in both study regions. To determine strength of the surface process contributions to these droughts, we examine the potential evaporation (E). For the NA, the average P-E (Table 2) was $-10.9 \text{ mm day}^{-1}$ in extreme dry summers and the average P anomaly was -3.9 mm day^{-1} . Thus, the maximum E anomaly was 7 mm day^{-1} . For moderate drought, the P-E anomaly was -6.5 mm day^{-1} , and the maximum E was 3.7 mm day^{-1} . Thus, the extreme dry summer E was larger in an absolute sense and relative to the P – E anomaly. This suggests the extreme droughts were driven more by surface processes. In the EE/WR, the mean P – E values were -9.9 mm day^{-1} and -6.4 mm day^{-1} for extreme and moderate dry summers respectively. Using the P (Table 5) suggests a similar result (maximum E of 6.4 and 4 mm day^{-1} , respectively). This is in spite of the fact 50% of these summers were not preceded by a dry spring.

4. Summary and Conclusions

Drought is a difficult and important topic to study as it is challenging to define precisely the time and space scales and because of the impact on agricultural and economic activity. Summer drought was examined for the agriculturally important regions of the central USA and Eastern Europe and Western Russia during the late 20th and early 21st centuries. Summer drought was defined as in [25] and section 2, which included a criterion to separate extreme dry summers from those of moderately dry summers. This study demonstrates the following results.

Summer drought within the agriculturally sensitive regions of NA and EE/WR occurred more often during the 1970s and the 2010s. Summers defined as extreme drought were accompanied by larger maximum P deficits and greater maximum E. The extreme drought years were accompanied also by E values were a greater percentage of the maximum P-E total. In the NA, extreme dry summers occurred more often during LN years while moderate drought occurred more often during EN years. The opposite was found within the EE/WR. The only result supported by statistical testing was the distribution of extreme summer drought in the NA, but this result was weak.

Examining the synoptic-dynamic character of the NA drought summers demonstrated these summers occurred in association with the more frequent occurrence of zonal NH flow regimes or ECMs (significant at $p=0.01$). Extreme dry summers were separated from moderate dry summers by significantly fewer and weaker blocking events ($p = 0.05$ and stronger) and a negative PNA regime. For extreme dry summers, the positive 500 hPa anomaly was located above the study region rather than to the west as for moderate drought years.

The synoptic-dynamic character of extreme drought within the EE/WR showed a very strong negative EU teleconnection pattern similar to quasi-stationary long period Rossby Wave Trains found in other regions of the world. These years were accompanied by significantly more blocking, although not necessarily stronger blocking events as well as relatively more meridional NH flow regimes or ECMs. For moderate drought years, there was significantly weaker and less blocking as well as a significantly more zonal NH flow.

In both regions, extreme dry summers were a continuation of the atmospheric flow regimes from the spring, whereas for moderate dry summers, the spring flow regime was different from the summer. In addition, for both regions, wet summers displayed synoptic-dynamic characteristics were either opposite in terms of the teleconnections or associated with more meridional (NA) or zonal (EE/WR) ECMs.

Acknowledgements

The authors would like to thank the anonymous reviewers for their comments which helped to make this a stronger contribution.

References

- [1] Wilhite D A 2000 Drought: A Global Assessment (London, Routledge) pp 752
- [2] Ahrens C D, Henson R *Meteorology Today: An Introduction to Weather, Climate, and the Environment 11th Ed.* (Cengage Learning)
- [3] Hu Q, Buyanovsky G 2003 Climate effects on corn yield in Missouri *J. Appl Meteorol* **42** 1626–1635
- [4] Mehta V M, Mendoza K, Daggupati P, Srinivasan R, Rosenberg N J, Deb D 2016 High resolution simulations of decadal climate variability impacts on water yield in the Missouri River Basin with the soil and Water Assessment Tool (SWAT) *J. Hydrometeorology* **17** 2455 – 2476
- [5] Namias J 1983 Some causes of the United States drought. *J. Clim. Appl. Meteorol.* **22** 30 – 39
- [6] Lupo A R and Bosart L F 1999 An analysis of a relatively rare case of continental blocking *Quart. J. Roy. Meteor. Soc.* **125** 107-138
- [7] Kung E C, Chern J-G 1995 Prevailing anomaly patterns of the Global Sea Surface temperatures and tropospheric responses *Atmósfera* **8** 99-114
- [8] Lupo A R, Kelsey E P, Weitlich D K, Davis N A and Market P S 2008 Using the monthly classification of global SSTs and 500 hPa height anomalies to predict temperature and

- precipitation regimes one to two seasons in advance for the mid-Mississippi region *National Weather Digest* **32(1)** 11-33
- [9] Birk K, Lupo A R, Guinan P E, Barbieri C E 2010 The interannual variability of midwestern temperatures and precipitation as related to the ENSO and PDO *Atmosfera* **23** 95 – 128
- [10] Henson C B, Lupo A R, Market P S and Guinan P E 2017 ENSO and PDO-related climate variability impacts on Midwestern United States crop yields *Int. J. Biometeor.* **61** 857-867 DOI 10.1007/s00484-016-1263-3
- [11] Ionita M, Dima M, Nagavciuc V, Scholz P and Lohmann G 2021 Past megadroughts in central Europe were longer, more severe, and less warm than modern droughts *Nature Comm. Earth Env.* <https://doi.org/10.1038/s43247-021-00130-w>
- [12] Jaagus J, Aasa A, Aniskevich S et al. 2021 Long-term changes in drought indices in eastern and central Europe *J. Clim.* **34** [https://DOI: 10.1002/joc.7241](https://doi.org/10.1002/joc.7241)
- [13] Cherenkova E, Semenova I, Bardin M and Zolotokrylin A N 2015 Drought and grain crop yields over the East European Plain under influence of quasibiennial oscillation of global atmospheric processes *Int. Journ. Atmos. Sci.* **932474** 11 DOI:10.1155/2015/932474
- [14] Lupo A R, Mokhov I I, Chendev Y G, Lebedeva M G, Akperov M G 2014 Hubbard, Studying summer season drought in western Russia *Advances in Meteorology Special Issue: Large-scale Atmospheric Science, Anomalous Flows, and Teleconnections* **942027** 9
- [15] Lebedeva M G, Krymckaya O V, Lupo A R, Chendev Y G, Petin A N, Solovyov A 2016 Trends in summer season climate for Eastern Europe and Southern Russia in the early 21st century. *Advances in Meteorology Special Issue: Large Scale Atmospheric Science, Anomalous Flows, and Teleconnections 2015* **5035086** 10
- [16] Kononova N K 2009 *The Classification of Northern Hemisphere Circulation Mechanisms According to B.L. Dzerdzeevskii* (Izdatel'stvo "Voyentekhnizdat": Moscow, Russia)
- [17] Kononova N K 2015 Circulating epochs in the sectors of the Northern Hemisphere from 1899–2014 *Geopolit Ecogeodynamics Reg.* **11** 56–66
- [18] Dzerdzeevskii B L, Kurganskaya V M and Vitviskaya Z M 1946 The Classification of Circulation Mechanisms in the Northern Hemisphere and the Characteristics of Synoptic Seasons *In Synoptic Meteorology* (Gidrometizdat: Leningrad, Russia)
- [19] Kononova N K and Lupo A R 2020 Changes in the Dynamics of the Northern Hemisphere Atmospheric Circulation and the Relationship to Surface Temperature in the 20th and 21st Centuries *Atmosphere* **11** 14 doi:10.3390/atmos11030255.
- [20] Lebedeva M G, Lupo A R, Chendev Y G, Krymckaya O V and Solovyev A B 2019 Changes in the atmospheric circulation conditions and regional climatic characteristics in two remote regions since the mid-20th century *Atmosphere* **10** 11
- [21] Slizhe M, Semenova I, Pianova I, El Hadri Y 2018 Dynamics of macrocirculation processes accompanying by the dry winds in Ukraine in the present climatic period *Hrvatski Meteorološki časopis* **53(53)** 17-29 <https://hrcak.srce.hr/231265>
- [22] Semenova I and Slizhe M 2020 Synoptic conditions of droughts and dry winds in the Black Sea Steppe Province under recent decades *Front. Earth Sci.* **8** 69 doi: 10.3389/feart.2020.00069
- [23] Kalnay E, Kanamitsu M, Kistler R et al. 1996 The NCEP/NCAR 40-year reanalysis project. *Bull. Am. Meteorol. Soc.* **77** 437–471
- [24] University of Missouri Blocking Archive, 2021 <http://weather.missouri.edu/gcc/>
- [25] Lupo A R, Kononova N K, Semenova I G, Lebedeva M G 2021 A Comparison of the characteristics of extreme drought during the late 20th and early 21st centuries over Eastern Europe, Western Russia, and Central North America *Atmosphere* **12** P01033 pp 21
- [26] Lupo A R, Jensen A D, Mokhov I I, Timazhev A V, Eichler T and Efe B 2019 Changes in global blocking character during the most recent decades *Atmosphere* **10** ID 00092 pp 19
- [27] Nunes M J, Lupo A R, Lebedeva M G, Chendev Y G, Solovyov A B 2017 The occurrence of extreme monthly temperatures and precipitation in two global regions *Papers in Applied Geography* **3** 143-156 DOI: 10.1080/23754931.2017.1286253

- [28] National Oceanic and Atmospheric Administration (NOAA) Climate Prediction Center (CPC) Teleconnections https://www.cpc.ncep.noaa.gov/products/precip/CWlink/daily_ao_index/month_ao_index.shtml
- [29] Kononova N K Fluctuations in the Atmospheric Circulation of the Northern Hemisphere in the 20th and Early 21st Century <https://atmospheric-circulation.ru/>
- [30] Center for Ocean and Atmosphere Prediction Studies <http://www.coaps.fsu.edu>.
- [31] Ukraine: Agricultural Overview 2021 *World Data Center for Geoinformatics and Sustainable Development – WDC Ukraine* <http://wdc.org.ua/en/node/29>.
- [32] Dzerdzeevskii B L 1968 Circulation Mechanisms in the Atmosphere of the Northern Hemisphere in the Twentieth Century *In Materials of Meteorological Research; Institute of Geography of the USSR Academy of Sciences and the Interagency Geophysical, Committee under the Presidium of the USSR Academy of Sciences* (Moscow, Russia) pp 240
- [33] Wilks D S 2006 Statistical Methods in the Atmospheric Sciences *Int. Geophys Series number 91* (Academic Press: Cambridge, MA, USA) pp 627
- [34] Wang N and Zhang Y 2015 Evolution of Eurasian teleconnection pattern and its relationship to climate anomalies in China *Clim Dyn* **44** 1017–1028 DOI 10.1007/s00382-014-2171-z.
- [35] Barnston A G, Livesey R E 1987 Classification, seasonality and persistence of low-frequency atmospheric circulation patterns *Mon. Wea. Rev.* **115** 1083 – 1126